

Dynamics of mycelial aggregation in cultures of *Aspergillus oryzae*

A. Amanullah, E. Leonildi, A.W. Nienow, C.R. Thomas

101

Abstract Previous work has shown that in many mycelial fermentations the predominant morphological form is clumps (aggregates) which cannot be further reduced by dilution. During fermentation, the clump size and shape is affected by fragmentation, which in turn depends on agitation conditions. This paper addresses the question of whether mycelial aggregation can also occur during a fermentation. The dynamics of changes in mycelial morphology due to aggregation were investigated in 5.3-L chemostat cultures of *Aspergillus oryzae* by imposing a step decrease in agitation speed from 1,000 to 550 rpm under conditions of controlled non-limiting dissolved oxygen tension, with a steady-state biomass concentration of 2 g/L. The mean projected area (size) of the mycelia, measured using image analysis, increased from $5,300 \pm 400 \mu\text{m}^2$ (at 1,000 rpm) to $9,400 \pm 900 \mu\text{m}^2$ (at 550 rpm). This change occurred too rapidly for it to be solely caused by mycelial growth. Instead, it is proposed that the increase in size was indeed due to aggregation, probably due to physico-chemical affects such as hydrophobicity or charge interactions. Aggregation was also shown to occur in 4-L aerated batch cultures at higher biomass concentrations (5.3 and 11.2 g/L) in which the agitation speed was decreased from 1,100 to 550 rpm. Experiments were also conducted off-line in a mixing vessel in the absence of oxygen. In this case, aggregation was not observed. Thus, though the cause of aggregation at this stage is not clear, aerobic metabolism appears to be required.

1 Introduction

The industrial importance of filamentous fungi is illustrated by applications ranging across the production of antibiotics, organic acids, proteins and food. In many fungal fermentations the high apparent viscosities and the non-Newtonian behaviour of the broths necessitate the use of high agitation speeds to provide adequate mixing and

oxygen transfer. However, mycelial damage due to fragmentation is also possible at high stirrer speeds, and in some instances, this can lead to inferior product formation. For instance, Jüsten et al. [12] using *Penicillium chrysogenum* reported that agitation intensity strongly influenced penicillin production and it was suggested that this was due to breakage of the relatively weaker vacuolated regions of hyphae where penicillin synthesis appeared to be located. Similar results using *P. chrysogenum* were also reported by others [5, 14, 15, 19, 20, 27, 30]. On the other hand, recombinant protein production in chemostat cultures of *Aspergillus oryzae* was found to be independent of changes in agitation intensity and morphology [3]. Changes in mycelial morphology caused by agitation may also influence the rheology of fermentation broths [29], which in turn can affect fermenter bulk mixing and mass and heat transfer, with indirect effects on productivity.

Previous work has demonstrated that mycelial fragmentation due to mechanical forces mainly occurs in the high energy dissipation found in the impeller swept volume and is also dependent on the frequency at which the hyphae pass through this zone [3, 11, 12, 13]. These concepts are incorporated into the energy dissipation circulation function (EDC), or $[P/(kD^3t_c)]$, where P is the power input, D , the impeller diameter, t_c , the mean circulation time and k is a geometric constant for a given impeller. The EDC function has been used successfully to correlate mycelial fragmentation for different impeller types and agitation intensities [11, 12] and is also able to correlate mycelial fragmentation of other filamentous species [3]. In growing cultures at a given impeller speed, the morphology is determined by the balance of fragmentation and growth [3, 11], though it is possible that mycelial aggregation may also contribute. Although aggregation has been invoked as one possible way in which mycelia can increase their size [11], very little research on this topic has been reported. There is no detailed evidence in the literature as to whether mycelia aggregate or not following a reduction in the rate of agitation (an action which may be called for in a fermentation in response to a reduction in oxygen demand during a batch fermentation, for example). Though there is some indication of increases in clump size occurring in the work of Amanullah et al. [3], there is certainly no precise information on how quickly such a phenomenon occurs or on what causes the increase. Given the importance of mycelial morphology, it is important to understand the factors, including aggregation, that influence it.

Received: 10 February 2000 / Accepted: 25 January 2001

Published online: 17 August 2001

© Springer-Verlag 2001

A. Amanullah, E. Leonildi, A.W. Nienow, C.R. Thomas (✉)

Centre for Bioprocess Engineering,
School of Chemical Engineering,
The University of Birmingham, Edgbaston,
Birmingham B15 2TT, UK
E-mail: C.R.Thomas@bham.ac.uk

The aim of this study was to measure the dynamics of changes in mycelial morphology in response to a rapid and much reduced level of agitation intensity. This was investigated in chemostat cultures of *A. oryzae* by imposing a step decrease in agitation speed under conditions of controlled, non-limiting, dissolved oxygen tension (DOT). DOT control eliminated adventitious effects of changes in the dissolved oxygen concentration. Similar experiments were also conducted in batch cultures at higher biomass concentrations. Finally the same type of step decrease in agitation speed was imposed under oxygen limiting conditions by transferring broth from the batch fermentation to an off-line mixing vessel sparged with nitrogen.

2

Materials and methods

2.1

Media

2.1.1

Batch fermentation (in g/L)

Maltodextrin, 12.0; citric acid, 2.0; $\text{MgSO}_4 \cdot 7\text{H}_2\text{O}$, 2.0; KH_2PO_4 , 2.0; K_2SO_4 , 2.0; NH_4SO_4 , 3.0; CaCl_2 , 0.8; yeast extract, 5.0; trace metal solution (citric acid, 3.0; ZnSO_4 , 0.29; Fe_2SO_4 , 0.28; CuSO_4 , 0.25; MnSO_4 , 0.25; NiCl , 0.05) 0.5 mL/L; Pluronic P6100, 1.0 mL/L.

2.1.2

Continuous culture feed (in g/L)

Maltodextrin, 3.33; NH_4SO_4 , 8.0; K_2SO_4 , 1.5; $\text{MgSO}_4 \cdot 7\text{H}_2\text{O}$, 2.0; NaCl , 0.5; $\text{CaCl}_2 \cdot 2\text{H}_2\text{O}$, 0.1; trace metal solution (citric acid, 3.0; ZnSO_4 , 0.29; Fe_2SO_4 , 0.28; CuSO_4 , 0.25; MnSO_4 , 0.25; NiCl , 0.05) 1.0 mL/L; Pluronic P6100, 0.25 mL/L. The feed medium used in the chemostat contained an excess of all but one of the nutrients essential for growth. Maltodextrin, which has a low content of mono- and di-saccharides, was used as a limiting carbon source to control the steady-state biomass concentration.

2.2

Shake flask cultures

The recombinant strain of *A. oryzae* was supplied by Novo Nordisk A/S (Baegsvard, Denmark). Two 200-mL shake flasks were inoculated with a spore suspension and placed in an orbital shaker at 200 rpm and 30°C for 24 h. To avoid pellet formation, the initial batch medium was inoculated with a vegetative culture containing dispersed mycelia.

2.3

Chemostat cultures

Fermentations were conducted in a 6-L bioreactor (LSL Biolafitte, Luton, England) with a 5.3-L working volume (vessel diameter T , 150 mm; impeller diameter D , 75 mm). Agitation was provided by two Rushton turbines with a D/T ratio of 0.5. The lower impeller was $0.39T$ from the bottom of the vessel and the impeller spacing was equal to the vessel diameter. The culture was aerated at 0.5 vvm, the temperature was 32°C ($\pm 0.2^\circ\text{C}$), and the pH was 5.0 (± 0.05). Feeding began at 12 h (at the end of the batch phase) at a flow rate of 265 mL/h, resulting in a dilution

rate of 0.05 h^{-1} . The fermenter was operated as a constant mass chemostat. Further details can be found in Amanullah et al. [3].

Dissolved oxygen was measured by a polarographic probe (Ingold, Switzerland) and controlled at 75% ($\pm 1\%$) of air saturation by blending nitrogen with the inlet air using a gas blender. Thus the agitation speed could be varied without affecting either the dissolved oxygen concentration in the broth or aeration rate. The gassed power inputs were measured separately (in water) using a frictionless air-bearing dynamometer [21]. The agitation speed was maintained at 1,000 rpm (± 5 rpm) until 348 h when a morphological steady state had been obtained [3]. At this time, the speed was decreased to 550 rpm (± 5 rpm). The flow number of the Rushton turbines used for the calculation of mean circulation time and hence, EDC in the chemostat was 0.75. The agitation speeds of 1,000 and 550 rpm corresponded to gassed specific power inputs of 12 and 2.2 kWm^{-3} respectively and EDC values of 950 and $90\text{ kWm}^{-3}\text{s}^{-1}$ respectively. These agitation speeds were chosen to create a large decrease in the agitation induced fragmentation rate. Samples were taken for measurements of morphological parameters at 1, 5, 15, 30, 60 and 540 min after the speed reduction.

2.4

Batch and off-line cultures

The same bioreactor was used for batch fermentations, but the working volume was 4 L and there was only a single Rushton turbine ($D/T=0.5$). The operating temperature and pH were as before. The gassing rate was 1 vvm. The initial agitation speed was 1,100 rpm (gassed specific power input= 9.2 kWm^{-3} and $\text{EDC}=800\text{ kWm}^{-3}\text{s}^{-1}$). A sample was taken from the mid-exponential phase ($\mu=0.20\text{ h}^{-1}$) and the biomass concentration was determined as 5.3 g/L. Broth (1 L) was also transferred to an off-line, flat-bottomed, baffled, 1.4-L Electrolab P300 fermenter (Electrolab, Bredon, UK) (working volume=1 L, diameter=120 mm) giving an aspect ratio of 1. In the Electrolab, agitation was provided by a single $D/T=0.5$ Rushton turbine (flow number 0.75) and it was sparged with nitrogen at a rate of 1 vvm to simulate oxygen limited conditions. The transfer of broth from the 4-L fermentation was followed by an immediate decrease in the fermenter air-flow rate to maintain the gassing rate at 1 vvm and the agitation speed was reduced to 550 rpm (gassed specific power input= 1.1 kWm^{-3} and $\text{EDC}=50\text{ kWm}^{-3}\text{s}^{-1}$) in order to study any mycelial aggregation. Simultaneously, the agitation speed in the off-line vessel was set at 330 rpm to give an identical EDC to that in the fermenter (i.e. $\text{EDC}=50\text{ kWm}^{-3}\text{s}^{-1}$) at 550 rpm. The gassed power in the off-line vessel was determined from torque measurements [6] using a Visco-Mix (Coesfeld Messtechnik, Dortmund, Germany). The Visco-Mix was capable of measuring torque to $\pm 5\%$ even at this small scale. Samples were taken simultaneously from the fermenter and off-line vessel at 1, 5, 15, 30 and 60 min following the reduction in agitation intensity. These experiments allowed a comparison between changes in mycelial morphology in response to a lowering of agitation intensity in the presence and absence of oxygen at similar biomass concentrations.

The experiment described above was repeated with a higher biomass concentration (11.2 g/L) using broth from the late exponential phase ($\mu=0.15\text{ h}^{-1}$) to examine whether aggregation rates were dependent on biomass concentration.

2.5

Image analysis for the measurement of hyphal morphology

Samples were diluted 30 fold using 20% sucrose solution, fixed and stained using lactophenol cotton blue (Fluka Chemie, Buchs, Switzerland). This dilution, resulting in a typical biomass concentration of 0.2 g/L on the slide, was necessary to minimise any artefacts caused by hyphal overlapping. Mycelial morphology was measured using the method of Tucker et al. [28] on Quantimet 570 and Quantimet 600 image analysers (Leica, Cambridge, UK) connected to a Polyvar optical microscope (Reichert Jung Werke, Austria) and a Kodak microscope respectively. The magnification was 40 \times . A 30 μL aliquot from a previously Whirly-mixed vial was placed on a microscope slide and covered with a cover slip. Pipette tips with cut-off ends were used to dispense samples to eliminate preferential mycelial size selection during dilution and slide preparation. As a compromise between analysis time (typically between 2 and 3 h per sample) and accuracy of results, a total of 200 mycelia were analysed, including both clumps [23] and freely dispersed forms. Morphological parameters of interest for the freely-dispersed mycelia were mean total hyphal length, mean projected area and the number of tips per hypha. Clump morphology was quantified in terms of mean projected area [28]. The mean projected area of all the hyphal elements (clumps plus freely dispersed) was taken as a measure of the total biomass [22].

3

Results

3.1

Chemostat cultures

The mean projected area considering both the clumped and freely dispersed mycelia in the chemostat is shown in

Fig. 1. Statistical analysis showed that it was possible to obtain morphological steady states with respect to both mean projected area and mycelial size distribution [3]. Morphological measurements (projected area) of the biomass revealed that approximately $33\% \pm 2\%$ of the mycelia existed in the freely dispersed form at 1,000 rpm, with clumps accounting for the remainder (Fig. 2). The change in agitation speed to 550 rpm resulted in an initial rapid increase in the freely dispersed fraction to 42% (perhaps suggesting a rapid aggregation of the freely dispersed class), followed by a gradual decrease to a steady-state value of $15\% \pm 2\%$. The steady-state results (Fig. 2) also suggest that freely dispersed mycelia aggregate to form clumps.

Figure 3 shows the transient morphological data for all the mycelia in the chemostat experiment on an expanded scale. The mean projected area increased from $5,300 \pm 400\text{ }\mu\text{m}^2$ (at 1,000 rpm) to $9,400 \pm 900\text{ }\mu\text{m}^2$ (at 550 rpm) in just 1 h. The doubling time of the culture can be calculated as approximately 14 h at the specific growth rate of 0.05 h^{-1} . If it is assumed that fragmentation ceased following the change in agitation speed (this assumption is believed to be justified, given the significant lowering of the EDC), and that the density and width of the mycelia were constant, the measured changes would have required approximately 10 h if the increase in the mean projected area had been due to growth alone. This disparity suggests that some other process caused the rapid change in mycelial size.

The morphological transients of just the freely dispersed mycelia are shown in Fig. 4a and b. Figure 4a shows that a rapid increase in the mean total length from 380 ± 20 to $460 \pm 20\text{ }\mu\text{m}$ was measured only 1 min after the speed change with a change overall to $510 \pm 30\text{ }\mu\text{m}$ by 9 h. The mean number of tips (Fig. 4b) showed similar behaviour, increasing from 5.2 ± 0.5 to 7.2 ± 0.4 . These changes in the freely dispersed morphology were also too rapid for a biological response of the culture (i.e. due to hyphal extension and branching). This is demonstrated by the following calculation. Assuming that the hyphal diameter and density were constant, the mean tip extension rate [18, 20] can be calculated from:

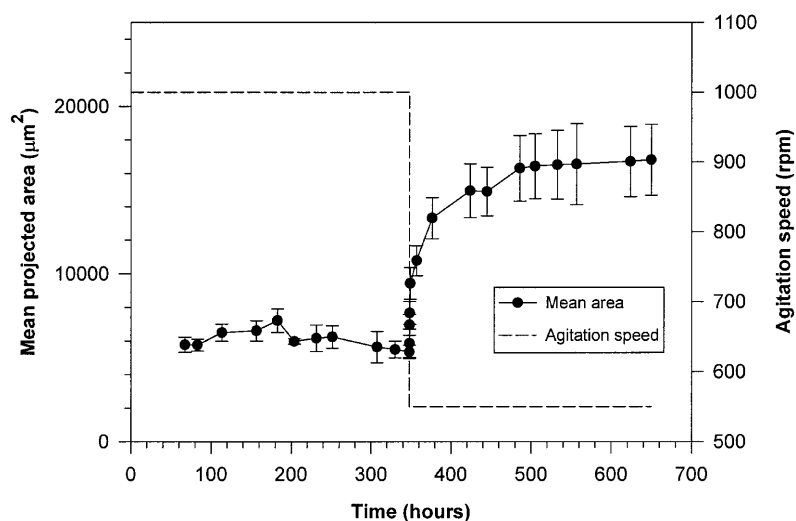


Fig. 1. The variation of mean projected area of the whole biomass in response to a lowering of agitation speed from 1,000 rpm ($\text{EDC}=950\text{ kWm}^3\text{s}^{-1}$) to 550 rpm ($\text{EDC}=90\text{ kWm}^3\text{s}^{-1}$) in a chemostat culture under conditions of controlled non-limiting dissolved oxygen

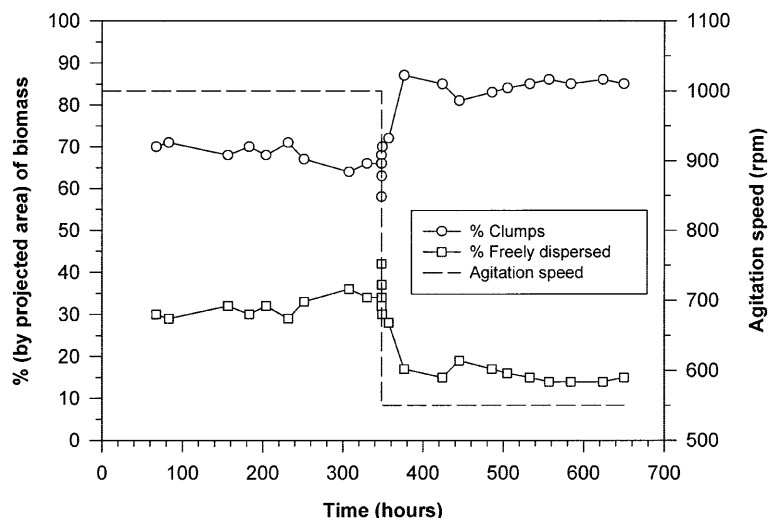


Fig. 2. The variation (%) of clumps and freely dispersed mycelia in response to a lowering of agitation speed from 1,000 rpm ($EDC=950 \text{ kWm}^3\text{s}^{-1}$) to 550 rpm ($EDC=90 \text{ kWm}^3\text{s}^{-1}$) in a chemostat culture under conditions of controlled non-limiting dissolved oxygen

$$r_{\text{tip}} = \mu \frac{L_t}{N_t} \quad (1)$$

where r_{tip} is the tip extension rate, μ , the specific growth rate, L_t , the mean total length and N_t , the mean number of tips per hypha. The above equation is strictly only valid for freely dispersed mycelia that do not undergo fragmentation, which is reasonable in the present circumstances. The application of Eq. (1) also assumes that the freely dispersed class is not contaminated by fragments breaking off clumps – again a reasonable assumption here. The mean tip extension rate calculated using Eq. (1) immediately preceding the step change in impeller speed was $3.7 \mu\text{m}/\text{tip}/\text{h}$. This implies that approximately 3.8 h would be required to account for the measured increase in mean total length, whereas most of the changes occurred in less than 1 h. Even if the assumption that the freely dispersed mycelia do not undergo fragmentation is incorrect, and in fact they are fragmented, there would be an even slower increase in the mean total length.

3.2

Batch and off-line cultures

Figure 5 shows the effects of lowering EDC from 800 to $50 \text{ kW}/\text{m}^3\text{s}$ in the batch fermentation (non-limiting dissolved oxygen condition) and off-line vessel (limiting dissolved oxygen condition) at biomass concentrations of 5.3 (mid-exponential) and 11.2 g/L (late exponential). Since mycelial size is mainly a balance between agitation intensity, growth and (as seems likely following this work) aggregation, and since the agitation intensity was the same in both cases, the relatively lower value of the mean projected area (at $t=0 \text{ min}$) at the higher biomass concentration reflected the lower specific growth rate of the culture. In all cases, there was a small increase in the mean projected area after just 1 min, followed by a decrease by 5 min. Incidentally, similar very short-term effects were also measured in the chemostat experiment (Figs. 2, 3 and 4), and although difficult to explain, they consistently occurred in chemostat, batch and off-line cultures and did not appear to be sampling artefacts.

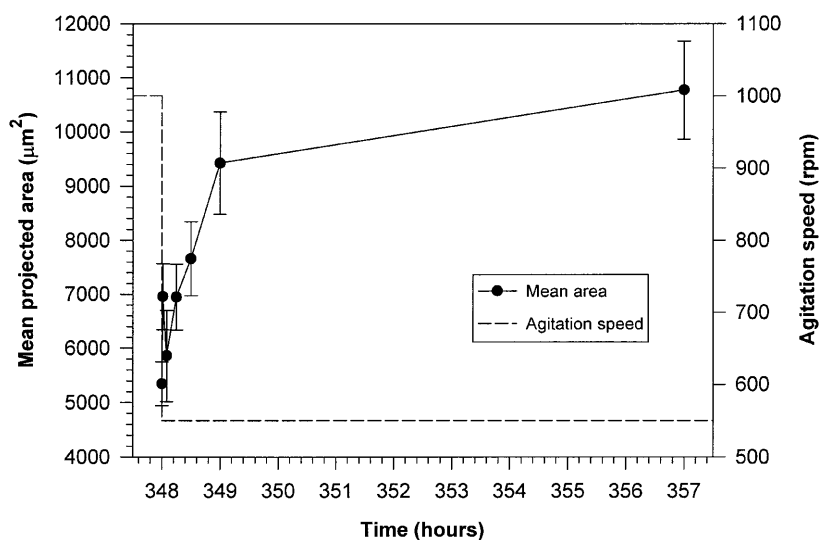


Fig. 3. Morphological transients of freely dispersed plus clumped mycelia in response to a lowering of agitation speed from 1,000 rpm ($EDC=950 \text{ kWm}^3\text{s}^{-1}$) to 550 rpm ($EDC=90 \text{ kWm}^3\text{s}^{-1}$) in a chemostat culture under conditions of controlled non-limiting dissolved oxygen

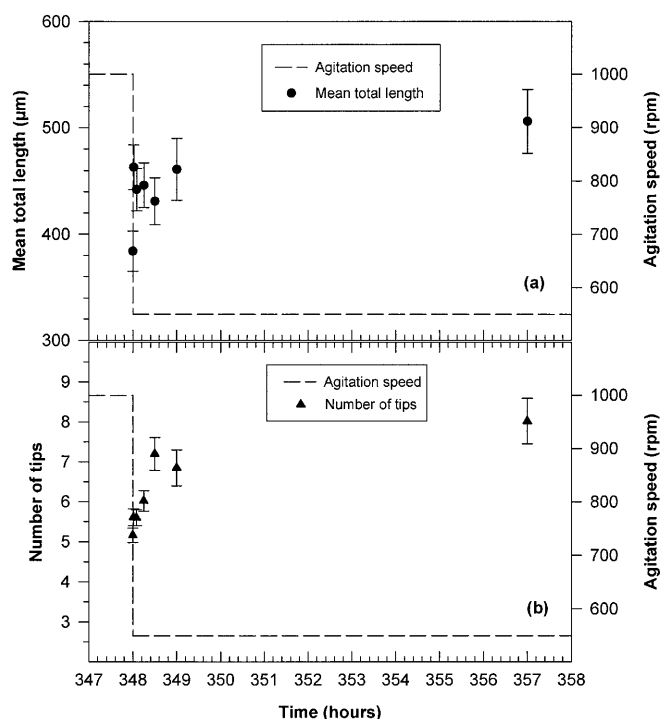


Fig. 4. Morphological transients of freely dispersed mycelia in response to a lowering of agitation speed from 1,000 rpm ($EDC=950 \text{ kWm}^3\text{s}^{-1}$) to 550 rpm ($EDC=90 \text{ kWm}^3\text{s}^{-1}$) in a chemostat culture under conditions of controlled non-limiting dissolved oxygen

The increase in mean projected area between 5 and 15 min was rapid and similar in magnitude (an increase of approximately 41% of the initial value) under aerobic conditions. The increase in mean projected area in this 10-min period was from $17,800 \pm 1,500 \mu\text{m}^2$ to $25,000 \pm 2,300 \mu\text{m}^2$ and from $12,000 \pm 1,300 \mu\text{m}^2$ to

$17,000 \pm 2,000 \mu\text{m}^2$ at biomass concentrations of 5.3 and 11.2 g/L respectively. If similar assumptions are applied to those for the chemostat morphological transient analysis, it can once again be shown that if mycelial growth alone was responsible, these changes would require between 85 and 115 min.

Finally, it can be seen in Fig. 5 that a significant increase in mean projected area was not measured in the absence of dissolved oxygen at either biomass concentration (Fig. 5). This result suggests that aggregation requires aerobic metabolism, even it is not the direct result of growth.

4 Discussion

The analysis of the transients of mycelial morphology in chemostat and batch cultures following a significant decrease in the rate of fragmentation show that the large increase in the mean projected area of the clumps plus freely dispersed mycelia cannot be explained by growth alone. Clearly a physical mechanism must have been responsible for the rapid increase in mean projected area and for the changes in the freely dispersed morphology. It is suggested that a physical mycelial aggregation process with a time constant of minutes caused the initial changes. It is also shown that the increase in the mean total length of the freely dispersed fraction is faster than the increase in the mean projected area of the clumps following the decrease in agitation speed. Although it is speculative, it appears that small hyphal elements have a greater tendency to aggregate than larger elements possibly due to their larger contact areas for ensuring stable contacts. However, it appears that such aggregation only occurs in cultures with the availability of dissolved oxygen, as there was no significant change in the morphology in off-line experiments where the broth was sparged with nitrogen.

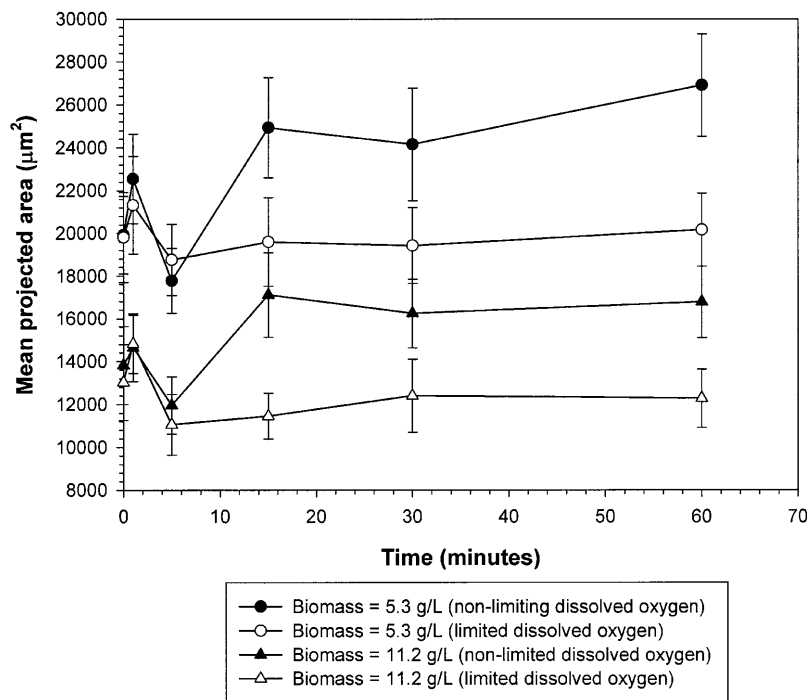


Fig. 5. Morphological transients of freely dispersed plus clumped mycelia at two different biomass concentrations in response to lowering EDC from 800 to $50 \text{ kWm}^3\text{s}^{-1}$ either when growing during a batch fermentation (non-limiting dissolved oxygen) or in an off-line mixing vessel under dissolved oxygen-limited conditions

Incidentally, aggregation in cultures of *P. chrysogenum* could not be measured either in similar off-line anaerobic experiments [11]. Possibly oxygen modifies the hydrophobicity of the mycelia, promoting aggregation. Vecht-Lifshitz and Braun [31] proposed that such hydrophobicity was biologically regulated by the supply of oxygen and mediated the aggregation of the filamentous bacterium *Streptomyces tendae*, and it is possible that similar phenomena occur in fungi. It is also interesting to note the role of mycelial growth on morphology in fed-batch cultures of *P. chrysogenum* [12] and *A. oryzae* [2] where extensive clump fragmentation occurs in the low specific growth rate fed-batch phase relative to the high specific growth rate batch phase.

The findings of this study are important since it is possible that in a large-scale fermentation, with long mean circulation times, mycelia aggregate rapidly outside the impeller swept volume after undergoing fragmentation within it. For instance, in a large-scale aerated bioreactor operated with a viscous mycelial fermentation, a mean circulation time between 20 and 60 s would be reasonable, and assuming that the circulation time can be described by a log normal distribution, they could in practice be distributed in the range 0–240 s (i.e. a maximum of a few minutes) [1]. This is the same order of magnitude as the times of the mycelial aggregation shown in Figs. 2, 3, 4 and 5. Thus, mycelia may be repeatedly fragmented and aggregated as they circulate through a large bioreactor. By the same reasoning, mycelial aggregation may not be as relevant in small bioreactors with very short circulation times. The knowledge of the dynamics of aggregation may also help to improve mathematical models describing mycelial morphology by incorporating the kinetics of fragmentation [12], growth [18] and aggregation.

The factors responsible for mycelial aggregation still remain largely unknown. For filamentous bacteria, it is thought that this probably occurs as a combination of both physical mycelial entanglement as well as due to charge effects on cell walls [31], although the mechanism is not well understood. The cell wall region is regarded as a crucial area responsible for aggregation with biofloculants [4, 16, 31]. Various charge effects, both polar and non-polar and of largely unknown origin (although often attributed to carboxyl groups and Ca^{2+}), can interact under favourable conditions to cause mycelial aggregation. These conditions may include strain type, dissolved oxygen [30], pH and ionic strength of medium [9, 10, 16, 25, 26], presence of surfactants or ion chelators in the medium [7, 8, 17], production of biofloculants [4], as well as the biomass concentration, the physiological state of the mycelia, collision frequency of mycelia and the agitation intensity [11].

A mechanism of microbial aggregation based on the presence of calcium ions in the medium has been proposed [17]. Calcium ions were thought to form a bridge between receptor sites (possibly carboxyl groups) on cell walls. The bonds formed are first ionic, but once established allow the cells to approach close to one another and therefore allow hydrogen bonding between complementary carbohydrate structures in the cell walls. It has been suggested that cellular aggregation can also result from the

interactions of extracellular polymers that accumulate at the microbial surface during growth [4]. These polymers combine either electrostatically or physically and bridge the cells in suspension. These authors stated that polymer bridging was probably the most likely cause of biological aggregates.

Realistically, due to the diversity in both environmental conditions of micro-organisms as well their cell wall properties, the exact mechanisms involved in the aggregation process remain largely unknown. Here it is proposed that aggregation is a two-step process and that aerobic metabolism is essential. The first step requires that mycelia have to approach and interact with each other, the precise mechanism by which they do so being very complex and unclear as discussed earlier, although the cell wall probably plays a crucial role. The second step involves physical entanglement with physico-chemical bonds sufficiently strong such that the resultant clumps that form cannot be disaggregated by dilution methods [22]. Such methods have been used extensively to ascertain clump and freely dispersed morphology and sizes throughout all of our work on mycelial fragmentation. Clearly, the stable clump structures of larger size following aggregation are not artefacts.

5

Conclusions

The dynamics of changes in mycelial morphology were investigated in chemostat and batch cultures of *A. oryzae*. The rapid increase in mean projected area of mycelial clumps following reductions in agitation speed was too rapid to be explained by growth alone and was due to aggregation. This aggregation process has a time constant of such a magnitude as to make it a likely occurrence during the passage of mycelia in the region away from the agitator in large-scale fungal fermentations. However, mycelial aggregation only occurred in aerobically metabolising cultures in the presence of dissolved oxygen and the exact factors responsible for the aggregation are far from clear. It is proposed that hydrophobicity and charges on cell walls play a crucial role, and which in turn appear to be strongly influenced by culture growth with the availability of dissolved oxygen.

References

1. Amanullah A, Baba A, McFarlane CM, Emery AN, Nienow AW (1993) Biological models of mixing performance in bioreactors. In: Proceedings of the 3rd International Conference on bioreactor and bioprocess fluid dynamics, 14–16 September 1993, University of Cambridge, UK. BHR Group/MEP, London, pp. 381–400
2. Amanullah A, Blair R, Nienow AW, Thomas CR (1998) Effects of agitation intensity on morphology and recombinant protein production in *Aspergillus oryzae*. In: Azevedo SF, Ferreira EC, Luyben KChAM, Osseweijer P (eds) European Symposium on biochemical engineering science 2, 16–19 September 1998, Porto, Portugal, pp 102–112
3. Amanullah A, Blair R, Nienow AW, Thomas CR (1999) Effects of agitation intensity on mycelial morphology and protein production in chemostat cultures of recombinant *Aspergillus oryzae*. Biotechnol Bioeng 62:434–446
4. Atkinson B, Daoud IS (1976) Microbial flocs and flocculation in fermentation process engineering. Adv Biochem Eng 4:41–124
5. Buckland BC, Gbewonyo K, Jain D, Glazomitsky K, Hunt G, Drew SW (1988) Oxygen transfer efficiency of hydrofoil impellers in

- both 800 L and 19,000 L fermenters. In: King R (ed) Proceedings of the 2nd International Conference on bioreactor fluid dynamics, BHRA/Elsevier, London, pp 1–15
6. Dyster KN, Koutsakos E, Jaworski Z, Nienow AW (1993) An LDA study of the radial discharge velocities generated by a Rushton turbine: Newtonian fluids, $Re \geq 3.5$. *Trans Inst Chem Engrs* 71:11–23
7. Elmayergi H, Scharer JM, Moo-Young M (1973) Effects of polymer additives on fermentation parameters in a culture of *A. niger*. *Biotechnol Bioeng* 25:845–859
8. Elmayergi H (1975) Mechanisms of pellet formation of *Aspergillus niger* with an additive. *J Ferment Technol* 53:722–729
9. Galbraith JC, Smith JE (1969) Filamentous growth of *Aspergillus niger* in submerged shake flask. *Trans Br Mycol Soc* 52(2): 237–246
10. Glazebrook MA, Vining LC, White RL (1992) Growth morphology of *Streptomyces akiyoshiensis* in submerged culture: influence of pH, inoculum and nutrients. *Can J Microbiol* 38:98–103
11. Jüsten P, Paul GC, Nienow AW, Thomas CR (1996) Dependence of mycelial morphology on impeller type and agitation intensity. *Biotechnol Bioeng* 52:634–648
12. Jüsten P, Paul GC, Nienow AW, Thomas CR (1998) Dependence of *Penicillium chrysogenum* growth, morphology, vacuolation and productivity in fed-batch fermentations on impeller type and agitation intensity. *Biotechnol Bioeng* 59:762–775
13. Jüsten P, Paul GC, Nienow AW, Thomas CR (1998) A mathematical model for agitation induced fragmentation of *P. chrysogenum*. *Bioproc Eng* 18:7–16
14. König B, Seewald Ch, Schügerl K (1981) Process engineering investigations of penicillin production. *Eur J Appl Microbiol Biotechnol* 12:205–211
15. Makagiansar HY, Shamlou PA, Thomas CR, Lilly MD (1993) The influence of mechanical forces on the morphology and penicillin production of *Penicillium chrysogenum*. *Bioproc Eng* 9:83–90
16. Metz B, Kossen NWF (1977) Biotechnology review : the growth of molds in the form of pellets – a literature review. *Biotechnol Bioeng* 19:781–799
17. Mill PJ (1964) The nature of the interactions between flocculent cells in the flocculation of *Saccharomyces cerevisiae*. *J Gen Microbiol* 35:61–68
18. Nielsen J (1992) Modelling the growth of filamentous fungi. *Adv Biochem Eng* 46:187–223
19. Nielsen J, Johansen CL, Jacobsen M, Krabben P, Villadsen J (1995) Pellet formation and fragmentation in submerged cultures of *Penicillium chrysogenum* and its relation to penicillin production. *Biotechnol Prog* 11:93–98
20. Nielsen J, Krabben P (1995) Hyphal growth and fragmentation of *Penicillium chrysogenum* in submerged cultures. *Biotechnol Bioeng* 46:588–598
21. Nienow AW, Miles D (1969) A dynamometer for the accurate measurement of mixing torque. *J Sci Instr* 2:994–995
22. Packer HL, Thomas CR (1990) Morphological measurements on filamentous micro-organisms by fully automatic image analysis. *Biotechnol Bioeng* 35:870–881
23. Paul GC, Thomas CR (1998) Characterisation of mycelial morphology using image analysis. *Adv Biochem Eng* 60:1–59
24. Pirt SJ, Callow DS (1959) Continuous flow culture of the filamentous mould *Penicillium chrysogenum* and the control of its morphology. *Nature* 184:307–310
25. Rizza V, Kornfeld JM (1969) Components of cell walls of *Penicillium chrysogenum*. *J Gen Microbiol* 58:307–315
26. Seviour RJ, Read MA Electrophoretic mobility of conidia of *Aspergillus niger* and the role of their surface properties in pelleting. *Trans Br Mycol Soc* 84:745–747
27. Smith JJ, Lilly MD, Fox RL (1990) Morphology and penicillin production of *Penicillium chrysogenum*. *Biotechnol Bioeng* 35:1011–1023
28. Tucker KG, Kelly T, Delgrazia P, Thomas CR (1992) Fully automatic measurement of mycelial morphology by image analysis. *Biotechnol Prog* 8:353–359
29. Tucker KG, Thomas CR (1993) Effect of biomass concentration and morphology on the rheological parameters of *Penicillium chrysogenum* fermentation broths. *Trans Inst Chem Engr C* 71:111–117
30. van Suidjam JC, Metz B (1981) Influence of engineering variables upon the morphology of filamentous molds. *Biotechnol Bioeng* 23:111–148
31. Vecht-Lifshitz SE, Magdassi S, Braun S (1990) Pellet formation and cellular aggregation in *Streptomyces tendae*. *Biotechnol Bioeng* 35:890–896